COMBINED IMPACT OF PRIMARY-SECONDARY RATIO AND EXCESS AIR ON COAL-FIRED POWER PLANT PERFORMANCE

Djarot B. Darmadi[1]*, Nurdin Hasananto Teguh[1], Lilis Yuliati[1], Eko Siswanto[1], Marco Talice[2]

[1] Mechanical Engineering Department, Faculty of Engineering, Brawijaya University, Malang, Indonesia
[2] PMSQUARED Engineering S.r.l.s, Cagliari, Italia

* b_darmadi_djarot@ub.ac.id

The primary-secondary air ratio is believed to impact both the combustion process and the overall performance of a power plant. This study aims to investigate how an increase in the primary-secondary air ratio affects the performance of a power plant located in north Gorontalo, South Sulawesi, Indonesia, using a GateCycle model. We conducted simulations of 48 variations based on three primary-secondary ratio values (PA-SA) to determine the optimal proportion of PA-SA. Our findings indicate that the optimal PA-SA ratio under stoichiometric conditions was 25-75%, resulting in a total cost of 108.03 million Rupiah per hour with a fuel burn rate of 22756 kg/h. When operating with 10% excess air, the optimal PA-SA ratio remains 25-75%, and the fuel flow and total cost were 22947 kg/h and 108.94 million Rupiah, respectively. Similarly, under 20% excess air, the optimal PA-SA ratio was also 25-75%, with a fuel flow rate and total cost of 23144 kg/h and 109.87 million Rupiah, respectively.

Keywords: primary air, secondary air, excess air, power plant, efficiency, GateCycle

1 INTRODUCTION

Human activities have had an increasing impact on the climate, resulting in an irreversible effect on both people and the climate system. One significant contributor to climate change is fossil fuel combustion, which releases large amounts of carbon dioxide into the environment [1]. The relationship between energy consumption and climate change has been widely studied in recent decades. However, the depletion of coal reserves has also been observed in several regions, particularly where coal-fired power plants are still the preferred choice in developed countries. This depletion is due to the unbalanced production of coal and the consumption of countries that heavily rely on coal. Coal consumption is forecasted to decline even further in the 2020s and 2040s, particularly if new power plants are not built [2] .

Indonesia is in the top ten coal consumers and heavily depends on coal-fired power plants due to their relatively low average cost compared to other power plant types [3]. However, the country is shifting towards renewable energy due to substantial regional coal demand, the growing domestic market, and the recent cuts in government subsidies for coal [4]. Fig. 1.A provides statistical data on coal demand and its share from 2000 until 2018 [5]. The Indonesian government has also been striving to improve the electrification ratio across all regions, as seen in Fig. 1.B depicting the electrification ratio in the year 2017, which shows that just a few Indonesian provinces have an electrification ratio above 95% while in some regions the ratio is as low as 48% circa. However, the increasing population growth and household formation in certain areas may hinder this ratio's progress, leading to a higher demand for electricity and an increased pace of coal depletion as mentioned earlier. Improving the efficiency of the existing coal-fired plant in Indonesia has become strategically important.
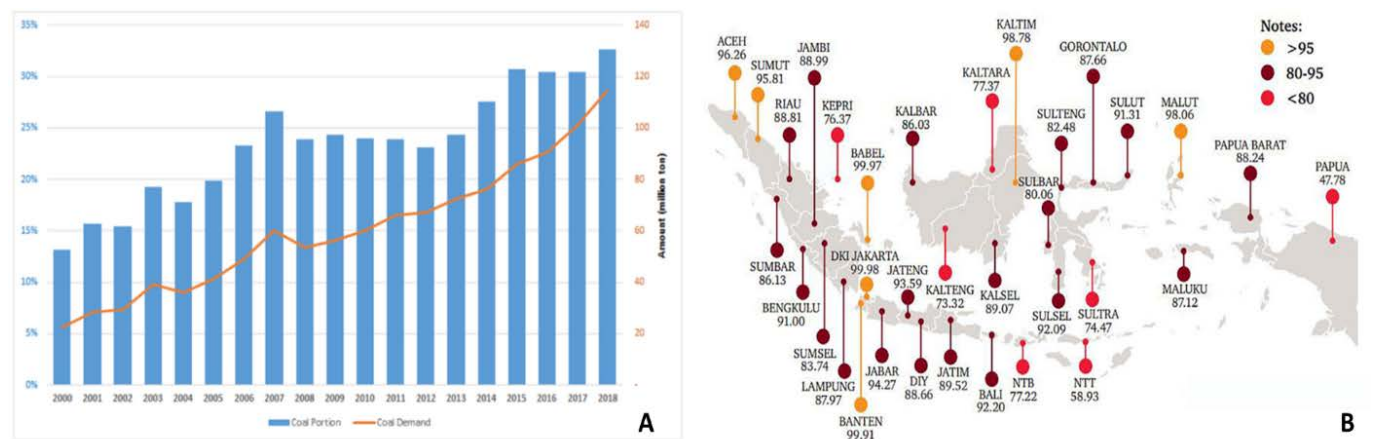

Fig. 1. (A) Indonesia's coal portion in the primary energy mix and coal demand [5] (B) Indonesia electrification ratio [6]

Efforts have been made to reduce coal usage through various means. One such approach is the preheating technology which reduces fuel consumption by shortening the combustion process time. Another solution is the use of high-efficiency combustion chambers, which can also minimize coal usage. A third option is to evaluate weekly or monthly volumetric usage. However, while high-efficiency combustion is beneficial, it may not be practical for power

Journal of Applied Engineering Science

Vol. 22, No. 1, 2022

www.engineeringscience.rs

iipp publishing

Djarot B. Darmadi et al. - Combined impact of primary-secondary ratio and excess air on coal-fired power plant performance

plants already in operation. While periodic cleaning can maintain energy conversion performance, it can also increase monthly expenses and decrease plant reliability.

A steam power plant comprises several primary components, including the turbine, condenser, FWH, pump, and boiler. Boilers facilitate two heat transfer processes: firstly, the energy stored in chemical form in the fuel is extracted through the combustion process into the furnace, and the resulting heat is transferred from the flue gas to water for phase change from water to steam. The resulting super-heated steam expands in a steam turbine coupled with a generator. In terms of flue gas, heat transfer occurs from the superheater to the air preheater. The air preheater (APH) is a critical piece of equipment in a coal-fired boiler power plant, designed to heat air and improve power plant performance while saving energy [7]. This equipment, along with the reheater, superheater, and economizer, is located in the convective section or back pass [8].

Boilers in power plants are operated in excess air conditions rather than stoichiometric conditions because it helps to ensure complete combustion of the fuel and reduces the emission of harmful pollutants. At stoichiometric conditions, the amount of supplied air is exactly equal to what is necessary for complete fuel oxidation. However, in reality, maintaining such conditions precisely is difficult. Even small variations in the fuel quality, temperature, pressure, or air supply can result in incomplete fuel combustion, leading to harmful pollutants formation, like carbon monoxide (CO), nitrogen oxides (NOx), and unburnt hydrocarbons.

On the other hand, when a boiler operates with excess air, more air is supplied than the theoretically required amount, ensuring that all the fuel is burned completely, and reducing the formation of harmful pollutants. However, operating with excessive air can result in higher fuel consumption and lower thermal efficiency. Therefore, a balance is sought between maintaining a sufficiently high excess air level to ensure complete combustion while minimizing excess air levels to improve thermal efficiency. The amount of excess air required can vary depending on several factors such as the type of fuel, boiler design, and operating conditions.

To improve combustion efficiency, and reduce pollutant formation, researchers have focused on ensuring reasonable air distribution in the furnace. Optimal overfire air (OFA) ratios can reduce NOx emissions while maintaining a stable carbon content in fly ash. Imbalances in air distribution in large-scale boilers can reduce efficiency and increase gas pollutant emissions, as noted in [9].Air distribution in a power plant involves primary and secondary air, each with different objectives. The primary air enters the lower part of the boiler and helps with the general flow circulation, as stated in [10]. It transports coal into the combustion chamber and is circulated and heated using the primary air fan and heater, respectively.

The use of secondary air is common in combustion processes [11]. However, primary and secondary air have different characteristics. Primary-air pressure is typically set to higher values because it needs to flow through more components [12]. In previous discussions, we talked about how power plants operate in excess air conditions. Maintaining the desired excess air value while achieving the target power output can be achieved by regulating either the quantity of air or fuel. In real-life situations, adjusting the airflow is more feasible than tuning the coal flow to meet the target excess air value and power output, as the calorific content of the coal type used daily in a power plant varies based on what is available in the market. There are different methods for regulating air including adjusting the primary-secondary air ratio for a given excess air value or changing the excess-air value while keeping the proportion between primary and secondary air unchanged. Both methods enhance the combustion process. In a study by [13] four primary-to-secondary-air-ratio scenarios were explored. The research found that increasing the ratio improved combustion stability and decreased NOx formation by up to 46% compared to the initial condition. In another study [10] , the combustion air ratio was 50% primary air, 45% secondary air, and 5% loop seal for solid recirculation purposes. Li et al. [14] examined the effect of the primary-air ratio on boiler performance and found that increasing the primary-air ratio caused coal combustion and boiler performance to decline. Primary-air flow determines the dense bed fluidization characteristics and the char particles' combustion reaction. At a lower primary-air airflow, the atmosphere in the dense bed is leaner in oxygen content, which does not facilitate the burning out of char. Moreover, a bed with a low temperature is not favorable for combustion [15]. Silva et al. [16] recorded primary-air flow fluctuation ranging from 34 to 54.10 m3/h and secondary-air flow rate varying from 10.85 to 26 m3/h within a 24-hour operation period. They also reported changes in the carbon-monoxide content, which fluctuated in a 200-400 mg/m3 range. Tong et al. [17] found a correlation between the excess-air coefficient (1-1.55) and the boiler efficiency when the plant was conducted with four different coals (anthracite, bituminous, lean coal, and lignite). Each coal had a different optimum value. Tong et al. reported that the highest boiler LHV (Lower Heating Value) efficiency was achieved when the excess air was 1.2 for anthracite and bituminous coal and 1.3 for lean coal and lignite. The similarity between the two excess-air values was justified by the fact that flue gas velocity reaches a point beyond which further increase is not favorable to burning coal particles. Ameri et al. [18] studied the influence of excess air at different load conditions (35, 50, 75, and 100%) on NOx production (PPmvd) and found that the NOx production rate increased as the excess air decreased. They also reported that the NOx production was maximum at the lowest load (35%). Based on their findings, they suggest operating the power plant at full load (100%). As no extensive research exists on the combined influence of primary-secondary ratio and excess air, we decided to explore this topic because it provides a wider range of possibilities for finding the optimum power plant performance.

Prior research on this subject has been conducted at a laboratory scale [19], which differs significantly from a full-scale power plant and requires careful consideration. While conducting experiments on a full-scale plant would provide more accurate results, it is expensive and poses higher risks for researchers due to the high pressure and

Journal of Applied Engineering Science

Vol. 22, No. 1, 2024

www.engineeringscience.rs

iipp
publishing

Djarot B. Darmadi et al. - Combined impact of primary-secondary ratio and excess air on coal-fired power plant performance

temperature levels. In contrast, small-scale power plants under 50,000 kW are considered safer and less complex to study, but there is a lack of research in this area [20].

Despite the significant research already conducted on the primary-secondary air ratio, a complete understanding of this subject matter has not yet been achieved, and many questions remain. This article aims to address two critical aspects: the role played by the PA-SA ratio and the impact of changing excess air on plant performance. Additionally, the paper will explore the effects of boiler air staging on an existing steam power plant, as excess air is one of the results of air staging. The hypothesis is that the plant's performance will increase up to a certain value of the PA-SA ratio and then decrease thereafter, while increased excess air may change the optimum volumetric airflow of primary-secondary air. This hypothesis will be tested by simulating a selected pool of parameters using the GateCycle software.

The research aims to find the optimum plant performance by changing the primary-secondary air ratio under stoichiometric conditions and different excess air values, with increments of 10%. The simplified model assumes a constant coal volumetric flow

2 EXPERIMENTAL SETUP

In this study, we utilized GateCycle software to create a model of a 25 MW steam power plant, whose performance was evaluated for different primary and secondary air ratios at three distinct values of the air-to-fuel ratio. We designed the power plant model to include multiple subsystems, such as coal combustion, steam generators, steam turbines with bleeding systems, feed water heaters, and the steam condensing system. Table 1 provides specifications of the coal used in the study, including its LHV (lower heating value) and proximate and ultimate analysis.

Table 1. Coal characteristics

Parameter of selected coal	Symbol	Unit	Value
Proximate Analysis			
Lower Heating Value	-	kJ/kg	14680.83
Temperature of coal	T_c	°C	27
Moisture level	M_{ar}	%	32.29
Ash content	A_{ar}	%	3.49
Carbon content	C_{ar}	%	31.2
Volatile matter content	Vm_{ar}	%	33.2
Ultimate analysis			
Solid a.r Carbon	C	fraction	0.2788
Solid a.r Hydrogen	H	fraction	0.0954
Solid a.r Oxygen	O	fraction	0.2348
Solid a.r Nitrogen	N	fraction	0.0049
Solid a.r Sulfur	S	fraction	0.0009
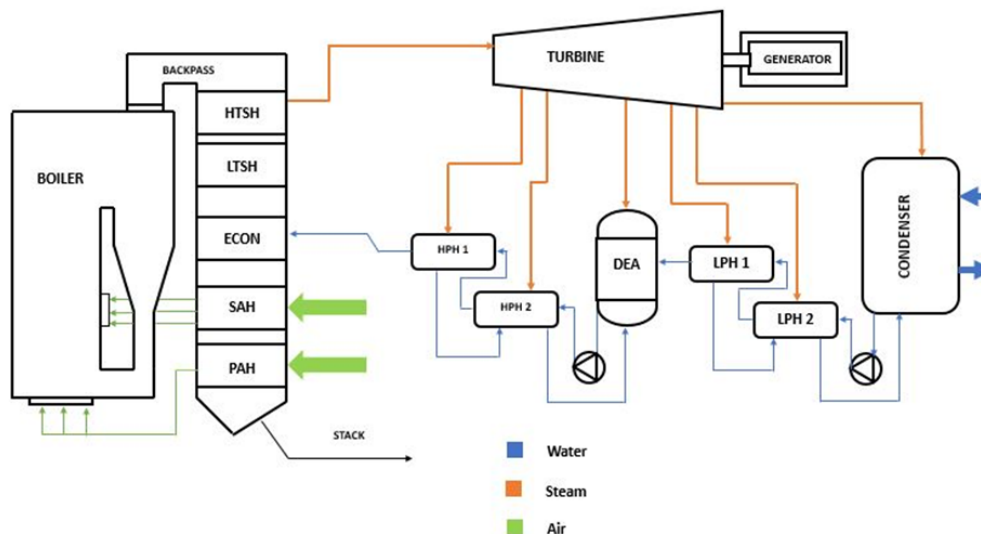
Fig. 2. Power plant scheme

Fig. 2. illustrates the power plant's schematic diagram. The steam is generated in a circulating fluidized bed boiler, using coal as fuel. The diagram depicts four feedwater heater stages, two of which are low-pressure heaters (LPH) and the other two are high-pressure heaters (HPH). Two pumps are located before the high-pressure heater number 2 and the low-pressure heater number 2. The backpass section of the steam generator includes a high-temperature

Journal of Applied Engineering Science

Vol. 22, No. 1, 2022

www.engineeringscience.rs

iipp
publishing

Djarot B. Darmadi et al. - Combined impact of primary-secondary ratio and excess air on coal-fired power plant performance

superheater, a low-temperature superheater, and an economizer. The study's primary focus, the secondary and primary air heaters, are positioned in the boiler backpass section, between the economizer and the stack. The main steam flow is then directed to the steam turbine to generate mechanical energy, which the generator converts into electrical energy. The steam turbine features five extraction points at various pressures, employed for heating fluids in the low-pressure heater, high-pressure heater, and deaerator. Different line colors in the figure correspond to different working fluids, with orange indicating a steam stream, and blue representing a water stream.

Fig. 3. displays the GateCycle model of the steam power plant operating in off-design conditions. Specifically in the case of water heaters, the off-design condition pertains to a state where the surface area remains unchanged, but the operating conditions can be altered [21]. This configuration allows for the exploration of plant improvement possibilities successfully. Laskowski et al. [22] employed this setup to assess the cooling process in the condenser, while Avagianos et al. [23] utilized it to evaluate the load in a Greek power plant. Moreover, Tong et al. [17]applied this approach to a 300 MW S-CO2 coal-fired boiler. Given its effectiveness, we adopt this setup for our study. The modeling outputs include the flue gas temperature, overall efficiency, air preheater mass flow and enthalpy, and the pollutant content in the flue gas stream. Comparable output and software studies have been conducted by Domazetis et al. [24] . The air preheater's heat transfer duty is calculated by determining the difference in flue gas energy at the inlet-outlet sections. The energy for each stream is determined by multiplying their mass flow and enthalpy values. The power plant model is based on a constant power generation value of 25 MW, and we perform one hundred iterations for each simulation to enhance the accuracy of the results. In GateCycle, the level of accuracy depends on the number of iterations, and the iterative process stops when a convergence state is attained [25].
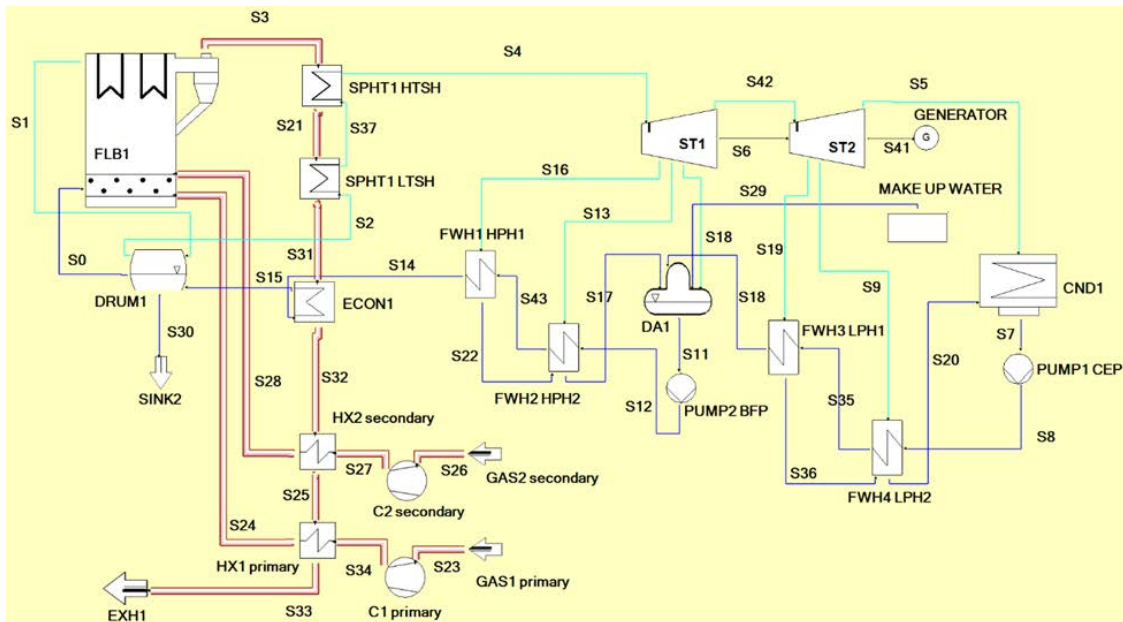
Fig. 3. GateCycle Model

This study utilized a research flowchart, as shown in Fig. 4., to investigate the effects of variations in PA-SA ratios and excess air modifications on power plant operation. These parameters were selected to explore a wide range of operating conditions, and Table 2 provides a detailed overview of the variations used. A total of 48 conditions were simulated to evaluate the combustion parameters and their impact on the working fluid. To further analyze the furnace performance, we conducted a statistical evaluation of changes in flue gas temperature at the back pass section. Additionally, the study includes a cost evaluation based on the different operating conditions. By integrating thermodynamic, economic, and environmental factors, we aimed to generate a comprehensive report for further research and operational evaluation.

Journal of Applied Engineering Science

Vol. 22, No. 1, 2024
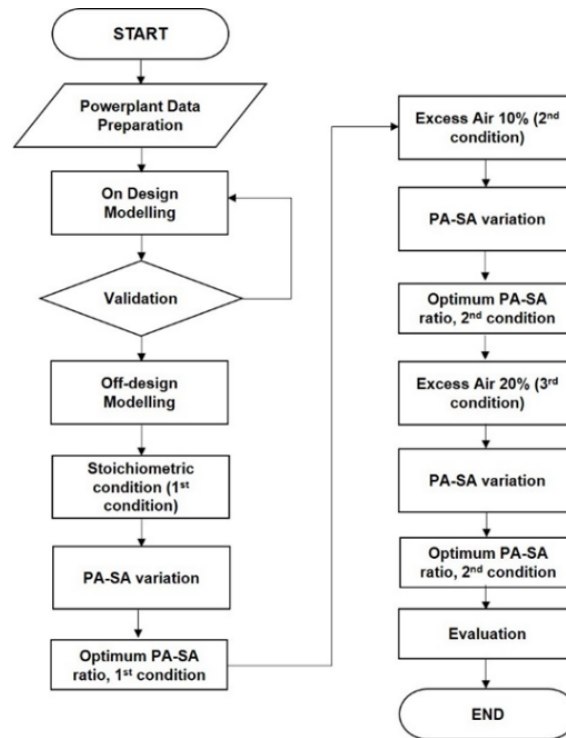*www.engineeringscience.rs*

iipp
publishing

Djarot B. Darmadi et al. - Combined impact of primary-secondary ratio and excess air on coal-fired power plant performance

Fig.4. Research flowchart

Table 2. Primary air secondary air ratio and Excess air variation

PA:SA ratio	Stoichiometric		10% Excess air		20% Excess air	
	Primary Air $\dot{m}\left(\frac{kg}{s}\right)$	Secondary Air $\dot{m}\left(\frac{kg}{s}\right)$	Primary Air $\dot{m}\left(\frac{kg}{s}\right)$	Secondary Air $\dot{m}\left(\frac{kg}{s}\right)$	Primary Air $\dot{m}\left(\frac{kg}{s}\right)$	Secondary Air $\dot{m}\left(\frac{kg}{s}\right)$
15:85	5.33	30.2	5.91	33.50	6.50	36.86
20:80	7.11	28.42	7.88	31.53	8.67	34.69
25:75	8.88	26.65	9.85	29.56	10.84	32.52
30:70	10.66	24.87	11.82	27.59	13.01	30.35
35:65	12.44	23.09	13.79	25.62	15.18	28.18
40:60	14.21	21.32	15.76	23.65	17.34	26.02
45:55	15.99	19.54	17.73	21.68	19.51	23.85
50:50	17.76	17,76	19.70	19.70	21.68	21.68
55:45	19.54	15.99	21.68	17.73	23.85	19.51
60:40	21.32	14.21	23.65	15.76	26.02	17.34
65:35	23.09	12.44	25.62	13.79	28.18	15.18
70-30	24.87	10.66	27.59	11.82	30.35	13.01
75-25	26.65	8.88	29.56	9.85	32.52	10.84
80-20	28.42	7.11	31.53	7.88	34.69	8.67
85-15	30.20	5.33	33.50	5.91	36.86	6.50
90-10	31.98	3.55	35.47	3.94	39.02	4.34

3 GOVERNING EQUATION

Thermodynamic relationships govern all the various components of the power plant. Before analyzing the cycle and studying the effects of combustion parameter variations, it's helpful to recall the thermodynamic laws that form the basis of the study. If we neglect kinetic and potential energy, we can express the principle of mass conservation and the first law of thermodynamics for a standard control volume:

$$\sum m_{in} = \sum m_{out} \tag{1}$$

Where m_{in} and m_{out} represent the inlet and outlet mass flows, respectively. Application of the first law of thermodynamics yields:

$$W - Q = \sum m_{in}h_{in} - \sum m_{out}h_{out} \tag{2}$$

With reference to the subscripts of Fig. 3., the numbers used in the following equation refer to the corresponding streamline. The primary air heater (PAH) heat balance equation writes:

$$\sum m_{in} = \sum m_{out} \tag{1}$$

$$m_{34}h_{34} + m_{25}h_{25} = m_{24}h_{24} + m_{33}h_{33} \tag{3}$$

Journal of Applied Engineering Science

Vol. 22, No. 1, 2022

www.engineeringscience.rs

iipp
publishing

Djarot B. Darmadi et al. - Combined impact of primary-secondary ratio and excess air on coal-fired power plant performance

Secondary air heater (SAH) heat balance can be written as:

$$m_{27}h_{27} + m_{32}h_{32} = m_{25}h_{25} + m_{28}h_{28} \tag{4}$$

For calculating the primary air ratio, we first calculated the total airflow, the sum of the primary and secondary airflow. If we then take the proportion of the primary air flow compared to the total airflow, we obtain the primary air ratio. This can be written as:

$$\dot{m}_{air,total} = \dot{m}_{PA} + \dot{m}_{SA} \tag{5}$$

$$PA\_ratio = \frac{m_{PA}}{\dot{m}_{air,total}} \tag{6}$$

$$SA\_ratio = \frac{m_{SA}}{\dot{m}_{air,total}} \tag{7}$$

The Anggrek power plant is equipped with four feed water heaters, which comprise two low-pressure heaters and two high-pressure heaters. Specifically, in regard to low-pressure heater number 2, the following relationship yields:

$$m_8h_8 + m_9h_9 + m_{36}h_{36} = m_{35}h_{35} + m_{20}h_{20} \tag{8}$$

For low-pressure heater number 1, the energy balance is:

$$m_{35}h_{35} + m_{19}h_{19} = m_{18}h_{18} + m_{36}h_{36} \tag{9}$$

For high-pressure heater number 2, the energy balance can be written as in Teguh *et al.* [26]:

$$m_{12}h_{12} + m_{13}h_{13} + m_{22}h_{22} = m_{43}h_{43} + m_{17}h_{17} \tag{10}$$

For high-pressure heater number 1, the energy balance writes:

$$m_{43}h_{43} + m_{16}h_{16} = m_{14}h_{14} + m_{22}h_{22} \tag{11}$$

It is important to note that the equations mentioned above do not account for any energy loss factors, as indicated in reference [27]. Thus, if one considers the effects of heat transfer losses, slagging, and fouling, the resulting equations may differ. According to Khodaei *et al.* [19], the air-to-fuel stoichiometric ratio can be expressed as:

$$\lambda = \frac{\left(\left(\frac{A}{F}\right)\right)}{\left(\frac{A}{F}\right)_{stoic}} \tag{12}$$

$(A/F)\_stoic$ is computed from its definition, as reported, for example, in Hashmi *et al.* [28]:

$$\left(\frac{A}{F}\right)_{stoic} = \left(\frac{m_{air}}{m_{fuel}}\right)_{stoic} \tag{13}$$

The efficiency of a power plant can be defined as the ratio of the net mechanical work output to the heat input into the boiler. A higher efficiency value indicates the superior performance of the power plant. This relationship can be expressed as:

$$\eta = \frac{W_{nett}}{Q_{in}} \, x100\% \tag{14}$$

$$W_{nett} = W_T - W_{aux} \tag{15}$$

Another way to define the plant's performance is through its heat rate. In this case, a lower heat rate value indicates higher performance. The ratio between the energy input from fuel combustion and the produced electric energy defines the heat ratio [29]. The heat rate equation writes:

$$heat\ rate = \frac{Q_{in\,(kJ)}}{electrical\ energy\ (kWH)} \tag{16}$$

To evaluate costs, we are focusing solely on fuel expenses, which can be determined by multiplying the coal price by its consumption rate during a designated period. It's important to note that fuel prices can significantly fluctuate, and due to differences in industrial capacity, fuel consumption can also vary. Our model can incorporate other cost-related factors like electricity cost, carbon tax, and coal price, which are specific to the duration being assessed. The efficiency of the boiler is calculated by comparing the amount of energy inputted into the boiler to the resulting thermal energy output, as described in the equation presented by Hossain *et al.* [30]:

$$\eta_{boiler} = \frac{Boiler\ output}{Boiler\ input} \tag{17}$$

Journal of Applied Engineering Science

Vol. 22, No. 1, 2024

www.engineeringscience.rs

iipp
publishing

Djarot B. Darmadi et al. - Combined impact of primary-secondary ratio and excess air on coal-fired power plant performance

4   RESULT AND DISCUSSION

We conducted simulations of steam power plant performance to study the impact of the PA-SA ratio under forty-eight different conditions. Our results are presented through graphics that showcase power generation, flue gas temperature, and efficiency. To validate our model, we compared the simulated data with actual data and found that the difference is less than 2.5 percent, as shown in Fig. 5. and Table 4. Hence, we can confidently conclude that our model is valid.

4.1   Model validation

For model validation, researchers typically select a specific parameter to compare the simulated and actual data. For instance, Hashmi *et al.*[31] validated their model by comparing power output, while Li *et al.* [32] compared the distribution of gas-solid phases in the boiler, and Modliński *et al.* [33] used temperature as a validation indicator. In this study, we have chosen pressure as our validation indicator, similar to the approach taken by Akpan *et al.* [34]. To validate our GateCycle model, we compared the pressure values obtained from our model with those from the actual case. We set the maximum allowable difference or error to 2.5 percent. If the error is within this threshold, we can conclude that the model is valid. We provide details of our model validation in Table 3 and Fig. 5.

Table 3. Validation Model

Parameters	Code	Pressure								
		1st data	2nd data	3rd data	4th data	5th data	P avg	Dev.S (%)	Gatecycle	Error
ST1 [ST]: Steam Turbine										
Steam Inlet	S4_2	4911	4831	4931	4801	4311	4757	5.36	4757	0.01
First Extraction	S5_1	1741	1721	1691	1841	1801	1759	3.47	1759	0
Second Extraction	S6_1	1031	1021	1001	1131	1071	1051	4.9	1051	0
Third Extraction	S7_1	581	571	561	621	601	587	4.1	587	0
ST2 [ST]: Steam Turbine										
First Extraction	S9_1	171	171	171	181	181	175	3.13	175	0
Second Extraction	S10_1	81	81	71	81	81	79	5.66	79	0
Main Outlet (steam turbine)	S11	18.86	18.47	18.64	21.45	20.07	19	6.46	20	0.55
Main Exit (condenser)	S12_1	18.86	18.47	18.64	21.45	20.07	19	6.46	20	0.55
PUMP1 CEP [PUMP]: Pump										
Main Inlet	S12_2	18.86	18.86	18.64	21.45	20.07	20	6.08	20	0.1
Control Valve Outlet	S13_1	1301	1301	1291	1251	1201	1269	3.41	1261	0.6
FWH4 LPH2 [FWH]: Feedwater Heater										
Extraction Inlet	s10_2	81	81	71	81	81	79	5.66	79	0
Boiler Feed Water Inlet	S13_2	1301	1261	1291	861	1201	1183	15.57	1209	2.2
LPH1 [FWH]: Feedwater Heater										
Extraction Inlet	S9_2	171	171	171	181	181	175	3.13	175	0
DA1 [DEAER]: Deaerator										
Main Boiler Feed Water Inlet	S15_2	180.8	179.5	178.3	179.9	178.5	179	0.58	182	1.47
Main Boiler Feed Water Outlet	S16_1	191	181	181	171	181	175	4.04	178	1.7
PUMP2 BFP [PUMP]: Pump										
Main Inlet	S16_2	191	181	181	171	181	181	3.91	178	1.67
Control Valve Outlet	S17_1	8091	8091	7921	8031	7841	7995	1.38	7995	0
FWH2 HPH2 [FWH]: Feedwater Heater										
Extraction Inlet	S6_2	1031	1021	1001	1131	1071	1051	4.9	1051	0
Boiler Feed Water Inlet	S17_2	8091	8551	7921	8031	7841	8087	3.42	7995	1.14
FWH1 HPH1 [FWH]: Feedwater Heater										
Extraction Inlet	S5_2	1741	1721	1691	1841	1801	1759	3.47	1759	0
SPHT1 HTSH [SPHT]: Superheater										
Steam Outlet	S4_1	4921	4831	4931	4891	4311	4777	5.51	4757	0.42

Journal of Applied Engineering Science

Vol. 22, No. 1, 2022

www.engineeringscience.rs

iipp publishing

Djarot B. Darmadi et al. - Combined impact of primary-secondary ratio and excess air on coal-fired power plant performance
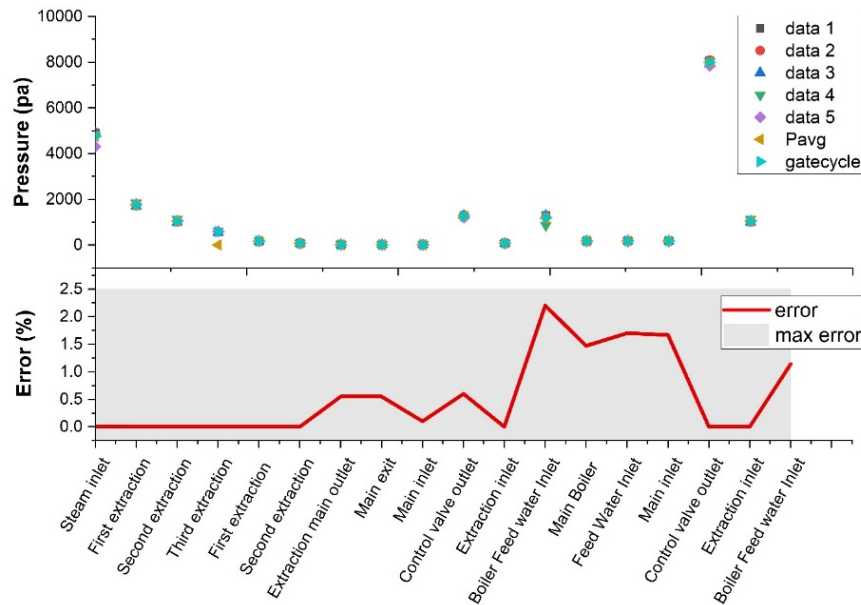
Fig. 5. Pressure-error graphic validation

4.2   Result

The data presented in Fig. 6. indicates that when operating under stoichiometric conditions (0% excess air), the efficiency of the plant generally increases as the volume of secondary air increases and the amount of primary air decreases. However, from the exam of the computed results one can see that the highest efficiency is achieved at around 75% secondary air and 25% primary air. As the proportion of secondary air increases beyond this point and the proportion of primary air decreases, the efficiency starts to decline. The figure also presents results for excess air levels of 10% and 20%. Similar to the stoichiometric case, the maximum efficiency is achieved at 25-75% secondary air for both excess air levels, beyond which the efficiency reduces. Next, we examine the impact of fuel flow.

In this part of the study, we aimed to maintain constant power generation while varying the PA-SA ratios and excess air. To achieve this, we adjusted the fuel flow rate, which became the dependent variable. Fig. 7. compares the fuel flow under three different conditions (stoichiometric, 10%, and 20% excess air) and reveals a similar trend in the fuel flow. In this context, fuel flow refers to the amount of coal inputted. The results show that the fuel flow slightly decreases for primary air values lower than 25% and then gradually increases as the primary air volume increases. As expected, higher excess air requires a higher volumetric coal flow to reach equivalent power generation. In stoichiometric conditions, fuel flow ranged from 22,756 kg/h to 23,502 kg/hour. At 10% excess air, fuel flow ranged from 22,947 kg/h to 23,771 kg/h, and for 20% excess air, fuel flows ranged from 23,144 kg/h to 24,019 kg/h. Fig. 8. also indicates that higher excess air and primary air ratios register wider gaps between maximum and minimum fuel flow. Gaps in stoichiometric, 10%, and 20% excess air conditions are 746 kg/h, 824 kg/h, and 975 kg/h, respectively. This finding suggests that using a higher amount of primary air leads to a higher combustion rate, which, in turn, requires more coal to burn.

Fig. 6. and 7. can be combined into a single Cartesian axis to provide a general overview of the relationship between efficiency and fuel flow at a certain excess air level. This is demonstrated in Fig. 8., which also displays the LHV energy input. A glance at Fig. 8. reveals that higher fuel flow results in greater power output, but lower efficiency. As previously mentioned, efficiency increases slightly from 15% PA to a maximum of 25%, while fuel flow exhibits the opposite trend. Fuel flow decreases slightly from 15% up to 25% PA, then increases rapidly as efficiency drops off sharply. Therefore, the efficiency trend is inversely related to the fuel flow trend. It should be noted that this model was created assuming equal power generation (25 MW). Based on GateCycle simulation, the optimal PA/SA for the Anggrek power plant is achieved at stoichiometric conditions with 25% primary air. In practice though, plants are never operated at stoichiometric conditions. Using non-zero excess air ensures complete combustion, but excessive excess air should be avoided to achieve maximum efficiency. The exact excess air value required for maximum efficiency is beyond the scope of this discussion and requires further research.

Fig. 9. illustrates the heat transfer that occurs in the primary and secondary air heaters under three distinct conditions. The trends in preheating and heat transfer differ between the two: the heat duty for primary air tends to increase, while the opposite is observed for secondary air. Specifically, the heat transfer duty for primary air heaters generally increases by almost twofold, while for secondary air, it drastically decreases. Based on these findings, we propose an evaluation that considers the optimum ratio for each condition.

We compared the optimal ratio for each excess air and observed a trend of decreasing temperature of the flue gas stream in the stack, as depicted in Fig. 10. It is noteworthy that the flue gas flow remained constant, and no gas leakage was modeled during this study. Specifically, we analyzed the heat transfer process of the flue gas across several equipment pieces, such as the HTSH (High-Temperature Super Heater), LTSH (Low-Temperature Super

Journal of Applied Engineering Science

Vol. 22, No. 1, 2024

www.engineeringscience.rs

iipp
publishing

Djarot B. Darmadi et al. - Combined impact of primary-secondary ratio and excess air on coal-fired power plant performance

Heater), Econ (Economizer), SAH (Secondary Air Heater), and PAH (Primary Air Heater). The flue gas temperature before entering the superheaters varied from 1005 to 1040 K depending on the excess air, as illustrated in Fig. 10. Under stoichiometric conditions, the flue gas temperature after passing through the high-temperature superheater, low-temperature superheater, economizer, secondary air heater, and primary air heater were 1040.4 K, 924.11 K, 819.75 K, 685 K, 592 K, and 572 K, respectively. With 10% excess air, the flue gas temperature after the high-pressure superheater, low-pressure superheater, economizer, secondary air heater, and primary air heater were 1021.96 K, 911.93 K, 811 K, 681.03 K, 588 K, and 569 K, respectively. Finally, with 20% excess air, the flue gas temperature after the high-pressure superheater, low-pressure superheater, economizer, secondary air heater, and primary air heater was 1005 K, 900.95 K, 804 K, 677 K, 585 K, and 566.61 K, respectively.

As the power plant studied is in Indonesia, the cost evaluation was carried out in the Indonesian rupiah (IDR). To calculate the fuel cost, we multiplied the plant's fuel consumption by the market coal price (USD 319/ton) per hour of operation and converted it into Indonesian rupiah using a conversion rate of 1 USD = IDR 14,882. We assumed that power generation would remain constant. Fig. 11. illustrates the fuel cost of the power plant concerning the primary-secondary air ratio and excess air. In stoichiometric conditions, fuel cost ranges from 108.03 to 111.57 million rupiahs per hour. With 10% excess air, the range is between 108.94 and 112.87 million rupiahs per hour. With 20% excess air, fuel cost ranges from 109.87 to 114.03 million rupiahs per hour. The model indicates that the highest expenditure is at 20% excess air and 90% primary air-10% secondary air, as the coal flow is higher than in any other condition, as previously mentioned while commenting on Fig. 9.
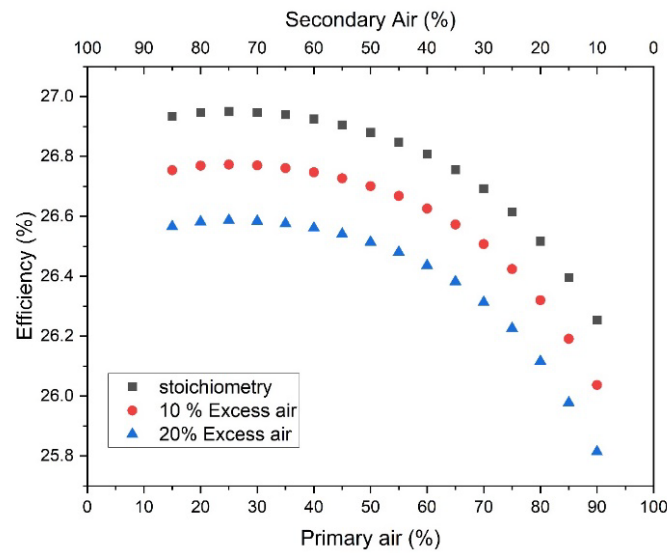
Fig. 6. Efficiency of power plant at different PA-SA and excess air

Fig. 7. Fuel flow at different excess air

Journal of Applied Engineering Science

Vol. 22, No. 1, 2022

www.engineeringscience.rs

iipp publishing

Djarot B. Darmadi et al. - Combined impact of primary-secondary ratio and excess air on coal-fired power plant performance

Fig. 8. Efficiency on different PA-SA ratio at (a) stoichiometric (b) 10% excess air (c) 20% excess air
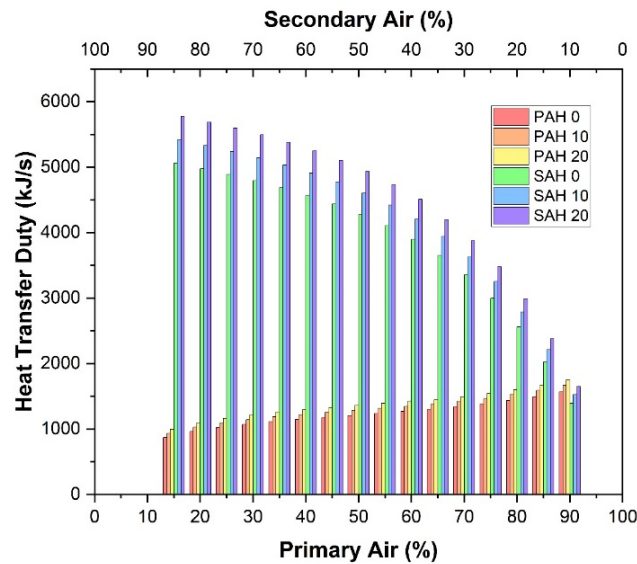
Fig. 9. Heat transfer of primary and secondary air heater at different PA-SA and excess air

Journal of Applied Engineering Science

Vol. 22, No. 1, 2024
www.engineeringscience.rs

iipp
publishing

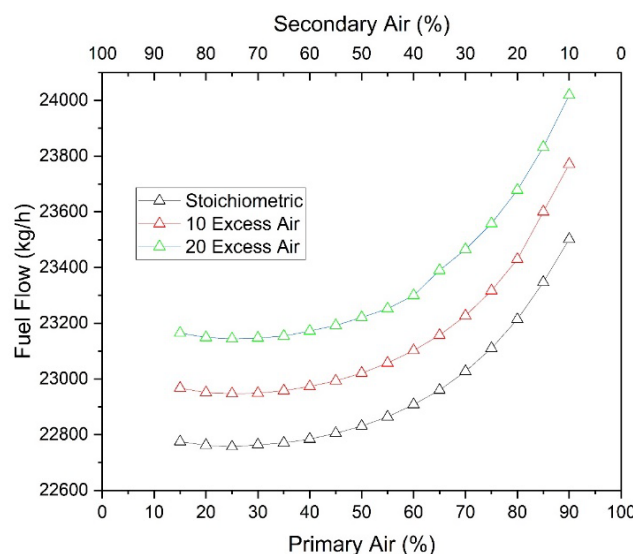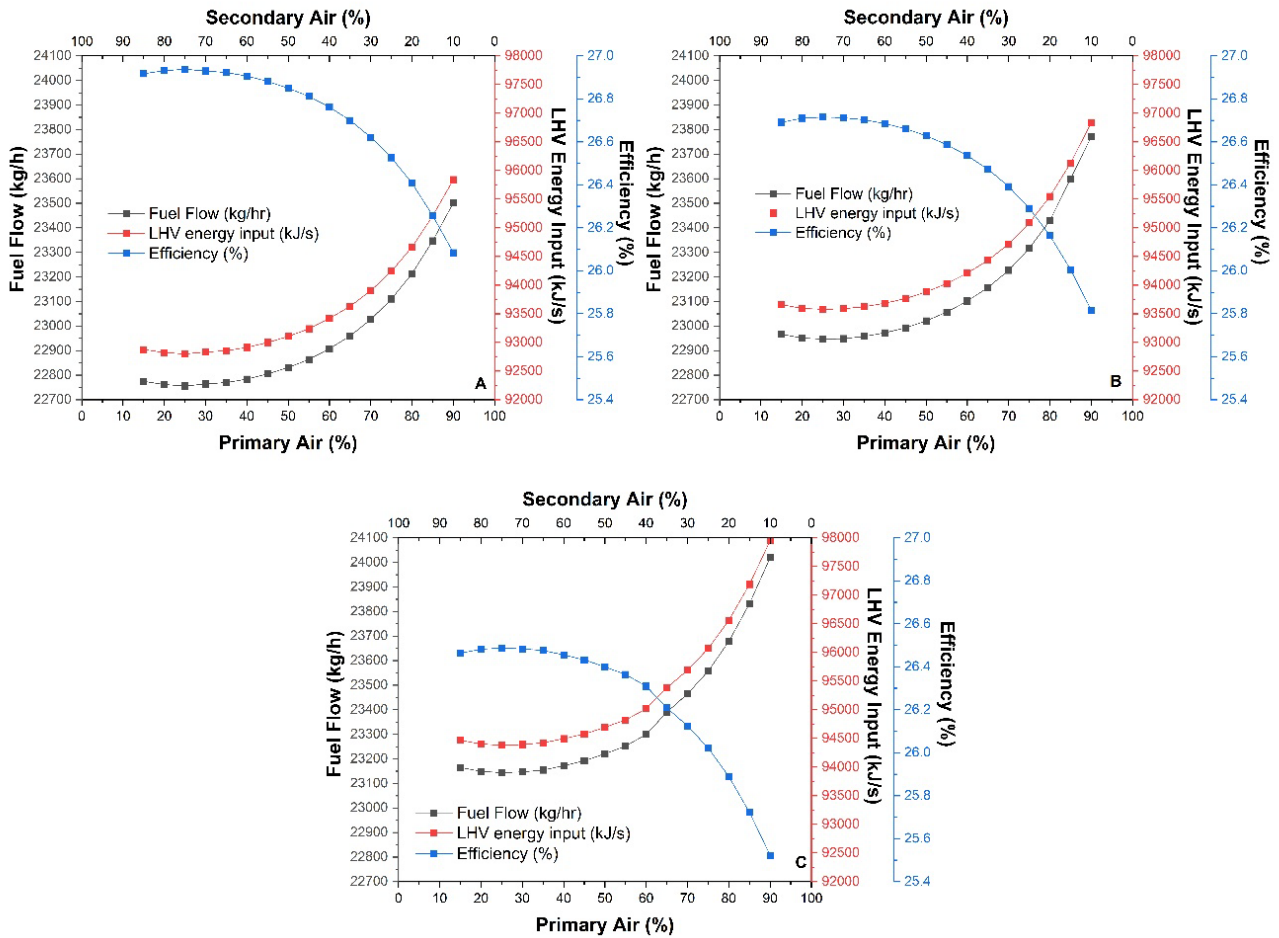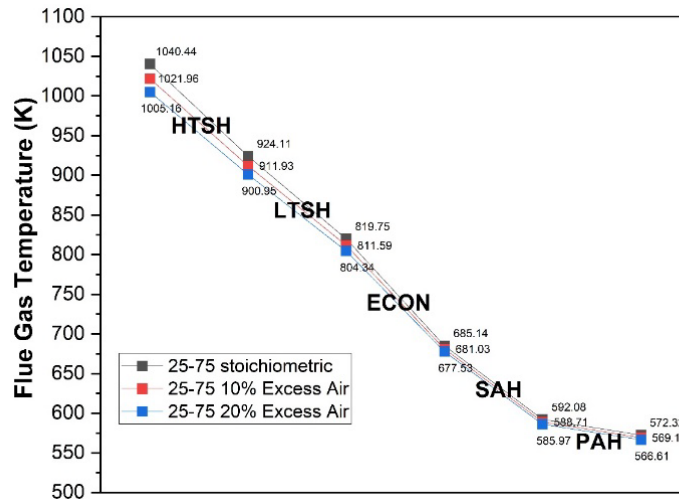*Djarot B. Darmadi et al. - Combined impact of primary-secondary ratio and excess air on coal-fired power plant performance*
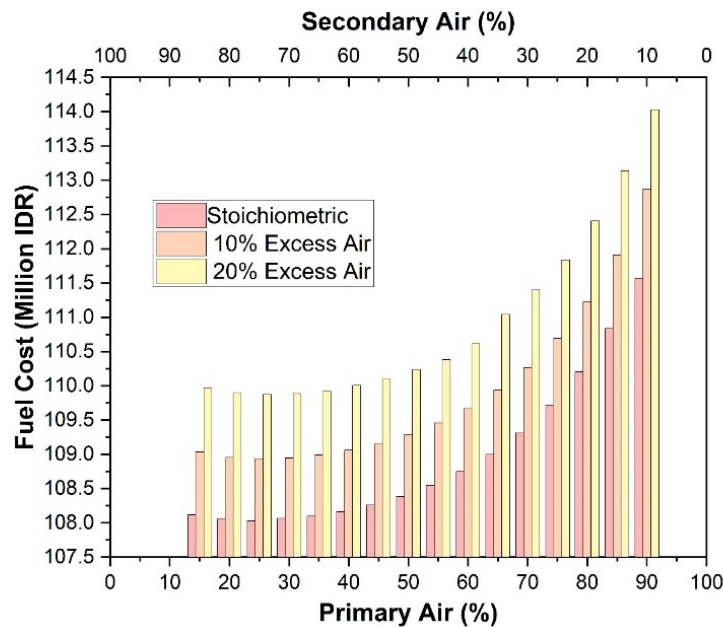
Fig. 10. Flue Gas Temperature Changes

Fig. 11. Coal cost at different conditions

4.3 Discussion

An electric power plant has the potential to use different types of chemical energy (fuel) to generate electric energy. However, the efficiency with which the plant converts the initial chemical energy into electric power is the key factor in assessing the plant's performance. In addition to efficiency, power generation, fuel flow, and fuel cost are important indicators for evaluating a power plant. In this study, we used efficiency as a measure of power plant output and to determine the optimal operating point. Power plant efficiency is a crucial metric for quantifying the conversion of heat from hydrocarbon combustion into electric energy [29]. Improved efficiency can lead to reduced fuel consumption and emissions, as well as lower operational costs and maintenance frequency. Simanjuntak *et al.* [35] reported similar results, suggesting that power plant performance declines after reaching the optimal condition, as the plant operates outside its design specification. As expressed in equation 14, power plant efficiency is the ratio of W_{nett} to Q_{in}. Given a constant generated power, this ratio depends solely on Q_{in}. We can calculate Q_{in} by multiplying the fuel's calorific value by its mass flow rate. Since we only considered one type of coal in our analysis, the results are subject to fluctuations in the coal flow rate.

Air is the primary mode of transporting and fluidizing coal after being heated by the primary air heater. The efficient operation of a power plant can be evaluated by determining boiler fuel flow [36]. At lower values of primary air, coal fails to mix sufficiently with secondary air, while higher primary air values increase fuel flow, which may reduce the possibility of insufficient mixing between coal and air. Higher fuel flow and coal quality also increase the energy input from the boiler [37]. Fig. 7. illustrates this. Residence time decreases as the primary air ratio increases under constant fuel flow conditions [38]. However, in our model, the increase in primary air is followed by a proportional increase in the fuel flow, which could alter the residence time. According to Jin *et al.* [38], the optimal value is between 0.123-0.153 of PAR or 12.3-15.3 percentile units. Oxygen availability is expected to aid in the carbon burnout of coal. As shown in Fig. 8., primary air worsens the combustion process and reduces combustion temperature beyond the

optimum conditions, as reported by Song *et al.* [39]. Fuel flow increases after surpassing 40 percent. Li *et al.* [40] conducted a study at 32.5 to 55 percent of PAR, indicating that higher PAR resulted in a significant increase in unburned carbon particles.

An air preheater is an essential component that facilitates the transfer of heat from hot flue gas to cold air. The efficiency of the energy transfer between two different working fluids is determined by various factors, including velocity, fluid properties, mass flow, temperature difference, and surface area. Since we conducted our study in off-design conditions, we kept the surface area constant. The primary air heater has a surface area twice as large as that of the secondary air heater. Heat transfer is significantly influenced by the ratio of primary air to secondary air [39]. In our study, we examined the distribution of primary and secondary air heaters for different ratios of total combustion air to analyze the impact of changes in the PA/SA ratio. From a thermodynamic standpoint, the heat transfer duty is closely linked to the flow and velocity of the fluid. A higher flow rate results in higher velocity values, which can affect the heat transfer process due to a causal relationship. While we found that an increase in excess air affects the secondary airflow, the primary air flow also changes proportionally. However, our results indicate a curve trend line instead of a linear dependence when the primary air-secondary air ratio is changed towards heat transfer duty. This is because of the difference in surface area, as shown in Fig. 9. The primary and secondary statistical trends have different inclinations, with primary air showing gradual increases and secondary air exhibiting sharp decreases.

After analyzing the different curve slopes in Fig. 10., it can be concluded that the economizer is where the highest heat transfer from flue gas to the steam line occurs. A study conducted by Avagianos et al. [23] had similar findings, but their work differs from the present study as their monitored power plant had two stages of reheaters, which affected the heat transfer process differently. Nonetheless, they found that the highest temperature changes were in the superheater. Similarly, in the Anggrek power plant, combining the low-pressure and high-pressure heaters would result in a higher temperature difference between the low and high superheaters compared to the economizer, with only a slight change in both air heaters.

5 CONCLUSIONS

After conducting a study on the effect of varying excess air and PA-SA ratios, the following results were obtained. By simulating multiple conditions and utilizing the GateCycle model, a specific optimum condition could be determined. It was found that at stoichiometric conditions, the optimum value is 25-75% of the PA-SA ratio, resulting in a cost expenditure of 108.03 million rupiahs and a coal flow rate of 22756 kg/h. For 10% excess air, the optimum value is also 25-75% of the PA-SA ratio, resulting in a cost expenditure of 108.94 million rupiahs and a coal flow rate of 22947 kg/h. For 20% excess air, the optimum value is 24-76% of the PA-SA ratio, resulting in a cost expenditure of 109.87 million rupiahs and a coal flow rate of 23144 kg/h. However, additional research or simulations should be conducted at varying load conditions and different excess air levels to provide more information on the optimal condition as a function of excess air and PA-SA ratio.

6 ACKNOWLEDGEMENT

7 REFERENCES

[1] M. Mohsin, S. Naseem, M. Sarfraz, and T. Azam (2022). Assessing the effects of fuel energy consumption, foreign direct investment and GDP on CO_2 emission: New data science evidence from Europe & Central Asia. Fuel, vol. 314, 15 April 2022, p. 123098, DOI: 10.1016/j.fuel.2021.123098.

[2] J. A. Ordonez, M. Fritz, and J. Eckstein (2022). Coal vs. renewables: Least-cost optimization of the Indonesian power sector. Energy for Sustain Development, vol. 68, pp. 350–363, DOI: 10.1016/j.esd.2022.04.017.

[3] F. R. Baskoro, K. Takahashi, K. Morikawa, and K. Nagasawa (2022). Multi-objective optimization on total cost and carbon dioxide emission of coal supply for coal-fired power plants in Indonesia. Socio-Economic Planning Sciences, vol. 81, June 2022, p. 101185, DOI: 10.1016/j.seps.2021.101185.

[4] R. Clark, N. Zucker, and J. Urpelainen (2020). The future of coal-fired power generation in Southeast Asia. Renewable and Sustain. Energy Reviews, vol. 121, April 2020, p. 109650, DOI: 10.1016/j.rser.2019.109650.

[5] F. R. Baskoro, K. Takahashi, K. Morikawa, and K. Nagasawa (2021). System dynamics approach in determining coal utilization scenario in Indonesia. Resour. Policy, vol. 73, October 2021, p. 102209, DOI: 10.1016/j.resourpol.2021.102209.

[6] Xuhua Kang, Jingchao Zhang, Huaming Zhang, Shenzhao Li, Yuzheng Zhang, Kai Zhang, Danqing Li (2021). Research on economic risk early-warning of China's overseas investment of coal-fired power generation: Take Indonesia as an example. Structural Change and Economic Dynamics, vol. 56, March 2021, pp. 298–309, DOI: 10.1016/j.strueco.2020.12.003.

Djarot B. Darmadi et al. - Combined impact of primary-secondary ratio and excess air on coal-fired power plant performance

[7] L. Wang, L. Deng, C. Tang, Q. Fan, C. Wang, and D. Che (2015). Thermal deformation prediction based on the temperature distribution of the rotor in rotary air-preheater. Applied Thermal Engineering, vol. 90, 5 November 2015, pp. 478–488, DOI: 10.1016/j.applthermaleng.2015.07.021.

[8] Y. Shi, J. Wen, F. Cui, and J. Wang (2019). An optimization study on soot-blowing of air preheaters in coal-fired power plant boilers. Energies, vol. 12, no. 5, pp. 1–15, DOI: 10.3390/en12050958.

[9] P. Madejski (2018). Numerical study of a large-scale pulverized coal-fired boiler operation using CFD modeling based on the probability density function method. Applied Thermal Engineering, vol. 145, 25 December 2018, pp. 352–363, DOI: 10.1016/j.applthermaleng.2018.09.004.

[10] P. Basu (2015), Circulating Fluidized Bed Boilers. Springer International Publishing, Canada. DOI: 10.1007/978-3-319-06173-3.

[11] R. Yan, Z. Chen, Y. Zheng, L. Yuan, L. Zeng, and Z. Li (2021). Influence of inner and outer secondary air ratio on flow and combustion characteristics of a swirl burner in a 29 MW pulverized coal boiler. Energy, vol. 237, p. 121625, DOI: 10.1016/j.energy.2021.121625.

[12] H. Chen, Z. Qi, L. Dai, B. Li, G. Xu, and Y. Yang (2020). Performance evaluation of a new conceptual combustion air preheating system in a 1000 MW coal-fueled power plant. Energy, vol. 193, 15 February 2020, p. 116739, DOI: 10.1016/j.energy.2019.116739.

[13] Qingxiang Wang, Zhichao Chen, Jiaquan Wang, Lingyan Zeng, Xin Zhang, Xiaoguang Li, Zhengqi Li (2018). Effects of secondary air distribution in primary combustion zone on combustion and NOx emissions of a large-scale down-fired boiler with air staging. Energy, vol. 165, Part B, 15 December 2018, pp. 399–410, DOI: 10.1016/j.energy.2018.09.194.

[14] Z. Li, Z. Miao, X. Shen, and J. Li (2018). Prevention of boiler performance degradation under large primary air ratio scenario in a 660 MW brown coal boiler. Energy, vol. 155, 15 July 2018, pp. 474–483, DOI: 10.1016/j.energy.2018.05.008.

[15] G. Qi, S. Zhang, X. Liu, J. Guan, Y. Chang, and Z. Wang (2017). Combustion adjustment test of circulating fluidized bed boiler. Applied Thermal Engineering, vol. 124, September 2017, pp. 1505–1511, DOI: 10.1016/j.applthermaleng.2017.07.005.

[16] J. P. Silva, S. Teixeira, É. Grilo, B. Peters, and J. C. Teixeira (2021). Analysis and monitoring of the combustion performance in a biomass power plant. Cleaner Engineering Technology, vol. 5, December 2021, p. 100334, DOI: 10.1016/j.clet.2021.100334.

[17] Y. Tong, L. Duan, and L. Pang (2021). Off-design performance analysis of a new 300 MW supercritical CO2 coal-fired boiler. Energy, vol. 216, 1 February 2021, p. 119306, DOI: 10.1016/j.energy.2020.119306.

[18] M. Ameri, H. Mokhtari, and M. Bahrami (2016). Energy, exergy, exergoeconomic and environmental (4E) optimization of a large steam power plant: A case study. Iranian Journal of Science and Technology, Transaction of Mechanical Engineering, vol. 40, Marc 2016, pp. 11–20, DOI: 10.1007/s40997-016-0002-z.

[19] H. Khodaei, F. Guzzomi, G. H. Yeoh, A. Regueiro, and D. Patiño (2017). An experimental study into the effect of air staging distribution and position on emissions in a laboratory scale biomass combustor. Energy, vol. 118, 1 January 2017. pp. 1243–1255, DOI: 10.1016/j.energy.2016.11.008.

[20] L. Malinowski, M. Lewandowska, and F. Giannetti (2017). Analysis of the secondary circuit of the DEMO fusion power plant using GateCycle. Fusion Engeneering and Design, vol. 124, November 2017, pp. 1237–1240, DOI: 10.1016/j.fusengdes.2017.03.026.

[21] K. C. Kushwaha and B. Koshti (2015). Performance Analysis and Off Design Behaviour of Feed Water Heater. International Journal of Research in Aeronautical and Mechanical Engineering, vol. 3, no. 10, pp. 9–15.

[22] R. Laskowski, A. Smyk, A. Rusowicz, and A. Grzebielec (2020). A useful formulas to describe the performance of a steam condenser in off-design conditions. Energy, vol. 204, 1 August 2020, DOI: 10.1016/j.energy.2020.117910.

[23] Ioannis Avagianos, Konstantinos Atsonios, Nikos Nikolopoulos, Panagiotis Grammelis, Nektarios Polonidis, Charalambos Papapavlou, Emmanuel Kakaras (2017). Predictive method for low load off-design operation of a lignite fired power plant. Fuel, vol. 209, 1 December 2017, pp. 685–693, DOI: 10.1016/j.fuel.2017.08.042.

[24] G. Domazetis, P. Barilla, B. D. James, and R. Glaisher (2008). Treatments of low rank coals for improved power generation and reduction in Greenhouse gas emissions. Fuel Processing Technology vol. 89, no. 1, pp. 68–76, 2007, DOI: 10.1016/j.fuproc.2007.07.004.

[25] X. Zhang, J. Yuan, Z. Tian, and J. Wang (2019). Estimation of the direct leakage of rotary air preheaters based on temperature distribution modeling. International Journal of Heat and Mass Transfer, vol. 134, May 2019, pp. 119–130, DOI: 10.1016/j.ijheatmasstransfer.2018.12.172.

[26] Nurdin Hasananto Teguh, Lilis Yuliati, and Djarot B. Darmadi (2022). Effect of seawater temperature rising to the performance of Northern Gorontalo small scale power plant. Case Studies in Thermal Engineering, vol. 32, April 2022, p. 101858, DOI: 10.1016/j.csite.2022.101858.

Journal of Applied Engineering Science

Vol. 22, No. 1, 2022

www.engineeringscience.rs

iipp publishing

Djarot B. Darmadi et al. - Combined impact of primary-secondary ratio and excess air on coal-fired power plant performance

[27] S. Chantasiriwan (2022). Improvement of conventional design of lignite-fired thermal power plant by integrating steam-air preheater and flue gas dryer," Energy Conversion Management: X, vol. 15, August 2022, p. 100272, DOI: 10.1016/j.ecmx.2022.100272.

[28] A. B. Al Hashmi, A. A. A. Mohamed, and Z. E. Dadach (2018). Process Simulation of a 620 Mw-Natural Gas Combined Cycle Power Plant with Optimum Flue Gas Recirculation. Open Journal of Energy Efficiency, vol. 07, no. 02, pp. 33–52, DOI: 10.4236/ojee.2018.72003.

[29] J. W. Burnett and L. L. Kiesling (2019). Power plant heat-rate efficiency as a regulatory mechanism: Implications for emission rates and levels. Energy Policy, vol. 134, November 2019, p. 110980, DOI: 10.1016/j.enpol.2019.110980.

[30] Shahariar Hossain, Hemal Chowdhury, Tamal Chowdhury, Jamal Uddin Ahamed, R. Saidur, Sadiq M. Sait, Marc A. Rosen (2020). Energy, exergy and sustainability analyses of Bangladesh's power generation sector. Energy Reports, vol. 6, November 2020, pp. 868–878, DOI: 10.1016/j.egyr.2020.04.010.

[31] M. B. Hashmi, M. A. A. Majid, and T. A. Lemma (2020). Combined effect of inlet air cooling and fouling on performance of variable geometry industrial gas turbines. Alexandria Engineering Journal, vol. 59, no. 3, pp. 1811–1821, DOI: 10.1016/j.aej.2020.04.050.

[32] Shuyue Li and Yansong Shen (2021). CFD investigation of maldistribution in a full-loop circulating fluidized bed with double parallel cyclones. Powder Technology, vol. 381, March 2021, pp. 665–684, DOI: 10.1016/j.powtec.2020.12.020.

[33] N. Modliński, K. Szczepanek, D. Nabagło, P. Madejski, and Z. Modliński (2019). Mathematical procedure for predicting tube metal temperature in the second stage reheater of the operating flexibly steam boiler. Applied Thermal Engineering, vol. 146, 5 January 2019, pp. 854–865, DOI: 10.1016/j.applthermaleng.2018.10.063.

[34] P. U. Akpan and W. F. Fuls (2019). Application and limits of a constant effectiveness model for predicting the pressure of steam condensers at off-design loads and cooling fluid temperatures. Applied Thermal Engineering, vol. 158, 25 July 2019, p. 113779, DOI: 10.1016/j.applthermaleng.2019.113779.

[35] M. E. Simanjuntak (2019). Pengaruh Excess Air Menggunakan Software. Rekayasa Mesin, vol. 10, no. 3, , pp. 287–298, DOI: 10.21776/ub.jrm.2019.010.03.9.

[36] D. Neshumayev, L. Rummel, A. Konist, A. Ots, and T. Parve (2018). Power plant fuel consumption rate during load cycling. Applied Energy, vol. 224, 15 August 2018, pp. 124–135, DOI: 10.1016/j.apenergy.2018.04.063.

[37] P. Rousseau and R. Laubscher (2020). Analysis of the impact of coal quality on the heat transfer distribution in a high-ash pulverized coal boiler using co-simulation. Energy, vol. 198, 1 May 2020, p. 117343, DOI: 10.1016/j.energy.2020.117343.

[38] Wei Jin, Fengqi Si, Sina Kheirkhah, Cong Yu, Hengyu Li, and Ya'ou Wang (2023). Numerical study on the effects of primary air ratio on ultra-low-load combustion characteristics of a 1050 MW coal-fired boiler considering high-temperature corrosion. Applied Thermal Engineering, vol. 221, 25 February 2023, p. 119811, DOI: 10.1016/j.applthermaleng.2022.119811.

[39] M. Song, L. Zeng, X. Yang, Z. Chen, and Z. Li (2018). Influence of the mass ratio of pulverized-coal in fuel-rich flow to that in fuel-lean flow on the gas/particle flow and particle distribution characteristics in a 600 MWe down-fired boiler," Experimental Thermal and Fluid Science, vol. 91, February 2018, pp. 363–373, 2018, DOI: 10.1016/j.expthermflusci.2017.07.006.

[40] Zixiang Li, Zhengqing Miao, Yan Zhou, Shurong Wen, and Jiangtao Li (2018). Influence of increased primary air ratio on boiler performance in a 660 MW brown coal boiler. Energy, vol. 152, 1 June 2018, pp. 804–817, DOI: 10.1016/j.energy.2018.04.001.

8 APPENDIX

8.1 Appendix 1. stoichiometric condition

Stream	From	To	Flow	Pressure	Temperature	Enthalpy	Quality
			kg/sec	kPa	K	kJ/kg	-
Fuel Gas Inlet	FLB1	FLB1	0	1378.9499	288.71	0	4
Cooling Water Inlet	CND1	CND1	1307.9848	172.3689	302.1868	121.7928	0
Cooling Water Exit	CND1	CND1	1307.9848	172.3689	311.7009	161.5439	0
Vent Steam Outlet	DA1	DA1	0.2313	177.97	389.7317	2701.04	1
S0	DRUM1	FLB1	113.4239	5087	538.141	1159.8948	0
S1	FLB1	DRUM1	113.4239	5087	538.141	1678.8131	0.3177
S10-S18	FWH3 LPH1	DA1	28.1156	425.3351	380.0688	448.502	0
S11	DA1	PUMP2 BFP	32.473	177.97	389.7317	489.2079	0
S12	PUMP2 BFP	FWH2 HPH2	32.473	7995.0001	390.7152	498.934	0
S13	ST1	FWH2 HPH2	1.3571	1051	487.8659	2859.5103	1
S14	FWH1 HPH1	ECON1	32.473	6398.89	447.2417	740.0458	0
S15	ECON1	DRUM1	32.473	5371.7218	497.5532	964.8117	0

Journal of Applied Engineering Science

Vol. 22, No. 1, 2024

www.engineeringscience.rs

iipp
publishing

Djarot B. Darmadi et al. - Combined impact of primary-secondary ratio and excess air on coal-fired power plant performance

Stream	From	To	Flow	Pressure	Temperature	Enthalpy	Quality
S16	ST1	FWH1 HPH1	2.3181	1759.0001	543.1216	2961.6796	1
S17	FWH2 HPH2	DA1	3.6751	1051	455.2069	772.2181	0
S18	ST1	DA1	0.3608	587	431.2639	2754.8355	1
S19	ST2	FWH3 LPH1	1.3196	175	389.2118	2569.5596	0.9409
S2	DRUM1	SPHT1 LTSH	32.1515	5087	538.141	2793.4984	1
S20	FWH4 LPH2	CND1	2.7026	79	366.3242	390.301	0
S21	SPHT1 HTSH	SPHT1 LTSH	41.4927	98.8449	924.1112	807.2008	0
S22	FWH1 HPH1	FWH2 HPH2	2.3181	1759.0001	479.1266	879.4217	0
S23	GAS1 primary	C1 primary	8.8743	110.655	316.95	29.138	1
S24	HX1 primary	FLB1	8.8743	113.9746	430.5301	147.047	1
S25	HX2 secon	HX1 primary	41.4927	98.8449	592.0885	368.4055	1
S26	GAS2 secondary	C2 secondary	26.6209	91.5408	313.95	26.0634	1
S27	C2 secondary	HX2 secon	26.6209	99.9625	321.8744	34.2529	1
S28	HX2 secon	FLB1	26.6209	99.9625	497.727	217.897	1
S29	MU1	DA1	0.5528	600	302.8	124.745	0
S3	FLB1	SPHT1 HTSH	41.4927	98.8449	1040.4461	969.9562	0
S30	DRUM1	SINK2	0.3215	5087	538.141	1159.8948	0
S31	SPHT1 LTSH	ECON1	41.4927	98.8449	819.7579	665.071	0
S32	ECON1	HX2 secon	41.4927	98.8449	685.1454	487.4059	0
S33	HX1 primary	EXH1	41.4927	98.8449	572.3218	343.5297	1
S34	C1 primary	HX1 primary	8.8743	113.9746	319.6148	31.8897	1
S35	FWH4 LPH2	FWH3 LPH1	28.1156	630.6625	357.0447	351.7262	0
S36	FWH3 LPH1	FWH4 LPH2	1.3196	175	389.2118	487.0023	0
S37	SPHT1 LTSH	SPHT1 HTSH	32.1515	4956.9528	588.6268	2975.1314	1
S4	SPHT1 HTSH	ST1	32.1515	4795.8337	665.4171	3183.0939	1
S41	ST2	GEN1	0	0	0	0	0.5
S42	ST1	ST2	28.1156	550	428.6178	2743.8023	0.9962
S43	FWH2 HPH2	FWH1 HPH1	32.473	7155.0593	412.9948	592.8763	0
S5	ST2	CND1	25.413	18.6262	331.7061	2275.5491	0.8596
S6	ST1	ST2	0	0	0	0	0.5
S7	CND1	PUMP1 CEP	28.1156	18.6262	331.7061	245.049	0
S8	PUMP1 CEP	FWH4 LPH2	28.1156	1261.325	331.8115	246.535	0
S9	ST2	FWH4 LPH2	1.3831	79	366.3242	2457.8103	0.9088
Expansion Line End	ST1	ST1	28.1156	550	428.6178	2743.8023	0.9962
Internal Pump Flow	PUMP1 CEP	PUMP1 CEP	28.1156	18.6262	331.7061	245.049	0
Internal Pump Flow	PUMP2 BFP	PUMP2 BFP	32.473	177.97	389.7317	489.2079	0
Expansion Line End	ST2	ST2	25.413	18.6262	331.7061	2275.5491	0.8596

8.2 Appendix 2 10% Excess air

Stream	From	To	Flow	Pressure	Temperature	Enthalpy	Quality
			kg/sec	kPa	K	kJ/kg	-
Fuel Gas Inlet	FLB1	FLB1	0	1378.9499	288.71	0	4
Cooling Water Inlet	CND1	CND1	1311.4499	172.3689	302.2358	121.9974	0
Cooling Water Exit	CND1	CND1	1311.4499	172.3689	311.7008	161.5439	0
Vent Steam Outlet	DA1	DA1	0.2298	177.97	389.7317	2701.04	1
S0	DRUM1	FLB1	113.4239	5087	538.141	1159.8948	0
S1	FLB1	DRUM1	113.4239	5087	538.141	1671.8052	0.3134
S10	FWH3 LPH1	DA1	27.9446	427.4957	380.1205	448.7218	0
S11	DA1	PUMP2 BFP	32.2717	177.97	389.7317	489.2079	0
S12	PUMP2 BFP	FWH2 HPH2	32.2717	7995.0001	390.7152	498.934	0
S13	ST1	FWH2 HPH2	1.3509	1051	492.0315	2869.4259	1
S14	FWH1 HPH1	ECON1	32.2717	6416.8827	447.521	741.2745	0
S15	ECON1	DRUM1	32.2717	5402.2832	500.4295	978.1363	0
S16	ST1	FWH1 HPH1	2.3023	1759.0001	547.6903	2972.5777	1
S17	FWH2 HPH2	DA1	3.6532	1051	455.2069	772.2181	0
S18	ST1	DA1	0.3544	587	435.0177	2763.7293	1
S19	ST2	FWH3 LPH1	1.3075	175	389.2118	2577.6578	0.9446
S2	DRUM1	SPHT1 LTSH	31.9522	5087	538.141	2793.4984	1
S20	FWH4 LPH2	CND1	2.6815	79	366.3242	390.301	0
S21	SPHT1 HTSH	SPHT1 LTSH	45.4187	98.8503	911.938	781.4276	0
S22	FWH1 HPH1	FWH2 HPH2	2.3023	1759.0001	479.1266	879.4217	0
S23	GAS1 primary	C1 primary	9.8437	110.655	316.95	29.138	1
S24	HX1 primary	FLB1	9.8437	113.9746	426.5581	142.8998	1
S25	HX2 secon	HX1 primary	45.4187	98.8503	588.715	360.2779	1
S26	GAS2 secondary	C2 secondary	29.5271	91.6925	313.95	26.0622	1
S27	C2 secondary	HX2 secon	29.5271	100.1282	321.8745	34.2515	1

Journal of Applied Engineering Science

Vol. 22, No. 1, 2022

www.engineeringscience.rs

iipp publishing

Djarot B. Darmadi et al. - Combined impact of primary-secondary ratio and excess air on coal-fired power plant performance

Stream	From	To	Flow	Pressure	Temperature	Enthalpy	Quality
S28	HX2 secon	FLB1	29.5271	100.1282	491.9524	211.7687	1
S29	MU1	DA1	0.5494	600	302.8	124.745	0
S3	FLB1	SPHT1 HTSH	45.4187	98.8503	1021.9656	932.901	0
S30	DRUM1	SINK2	0.3195	5087	538.141	1159.8948	0
S31	SPHT1 LTSH	ECON1	45.4187	98.8503	811.5944	646.82	0
S32	ECON1	HX2 secon	45.4187	98.8503	681.0388	476.8375	0
S33	HX1 primary	EXH1	45.4187	98.8503	569.1599	335.9778	1
S34	C1 primary	HX1 primary	9.8437	113.9746	319.6148	31.8897	1
S35	FWH4 LPH2	FWH3 LPH1	27.9446	630.6625	357.0788	351.8693	0
S36	FWH3 LPH1	FWH4 LPH2	1.3075	175	389.2118	487.0023	0
S37	SPHT1 LTSH	SPHT1 HTSH	31.9522	4958.5439	591.2921	2983.0101	1
S4	SPHT1 HTSH	ST1	31.9522	4798.2488	670.8137	3196.191	1
S41	ST2	GEN1	0	0	0	0	0.5
S42	ST1	ST2	27.9446	550	428.9951	2752.5984	1
S43	FWH2 HPH2	FWH1 HPH1	32.2717	7164.1499	413.1223	593.4261	0
S5	ST2	CND1	25.2632	18.592	331.6668	2282.3566	0.8625
S6	ST1	ST2	0	0	0	0	0.5
S7	CND1	PUMP1 CEP	27.9446	18.592	331.6667	244.8842	0
S8	PUMP1 CEP	FWH4 LPH2	27.9446	1261.325	331.7721	246.3703	0
S9	ST2	FWH4 LPH2	1.3739	79	366.3242	2465.4874	0.9122
Expansion Line End	ST1	ST1	27.9446	550	428.9951	2752.5984	1
Internal Pump Flow	PUMP1 CEP	PUMP1 CEP	27.9446	18.592	331.6668	244.8843	0
Internal Pump Flow	PUMP2 BFP	PUMP2 BFP	32.2717	177.97	389.7317	489.2079	0
Expansion Line End	ST2	ST2	25.2632	18.592	331.6668	2282.3566	0.8625

8.3 Appendix 3 20% Excess air

Stream	From	To	Flow	Pressure	Temperature	Enthalpy	Quality
			kg/sec	kPa	K	kJ/kg	-
Fuel Gas Inlet	FLB1	FLB1	0	1378.9499	288.71	0	4
Cooling Water Inlet	CND1	CND1	1309.5798	172.3689	302.247	122.0442	0
Cooling Water Exit	CND1	CND1	1309.5798	172.3689	311.7008	161.5438	0
Vent Steam Outlet	DA1	DA1	0.2285	177.97	389.7317	2701.04	1
S0	DRUM1	FLB1	113.4239	5087	538.141	1159.8948	0
S1	FLB1	DRUM1	113.4239	5087	538.141	1665.036	0.3092
S10	FWH3 LPH1	DA1	27.7811	429.5562	380.1686	448.9265	0
S11	DA1	PUMP2 BFP	32.0797	177.97	389.7317	489.2079	0
S12	PUMP2 BFP	FWH2 HPH2	32.0797	7995.0001	390.7152	498.934	0
S13	ST1	FWH2 HPH2	1.3451	1051	495.9603	2878.699	1
S14	FWH1 HPH1	ECON1	32.0797	6433.9529	447.7863	742.4415	0
S15	ECON1	DRUM1	32.0797	5431.2733	503.2583	991.2993	0
S16	ST1	FWH1 HPH1	2.2874	1759.0001	552.0017	2982.7792	1
S17	FWH2 HPH2	DA1	3.6324	1051	455.2069	772.2181	0
S18	ST1	DA1	0.3485	587	438.5518	2772.0333	1
S19	ST2	FWH3 LPH1	1.2964	175	389.2118	2585.1637	0.948
S2	DRUM1	SPHT1 LTSH	31.762	5087	538.141	2793.4984	1
S20	FWH4 LPH2	CND1	2.6626	79	366.3242	390.301	0
S21	SPHT1 HTSH	SPHT1 LTSH	49.4167	98.8366	900.9521	759.0479	0
S22	FWH1 HPH1	FWH2 HPH2	2.2874	1759.0001	479.1266	879.4217	0
S23	GAS1 primary	C1 primary	10.8308	110.655	316.95	29.138	1
S24	HX1 primary	FLB1	10.8308	113.9746	423.219	139.4063	1
S25	HX2 secon	HX1 primary	49.4167	98.8366	585.9717	353.5513	1
S26	GAS2 secondary	C2 secondary	32.4862	91.8386	313.95	26.0611	1
S27	C2 secondary	HX2 secon	32.4862	100.2877	321.8745	34.25	1
S28	HX2 secon	FLB1	32.4862	100.2877	486.988	206.5121	1
S29	MU1	DA1	0.5461	600	302.8	124.745	0
S3	FLB1	SPHT1 HTSH	49.4167	98.8366	1005.164	900.4677	0
S30	DRUM1	SINK2	0.3176	5087	538.141	1159.8948	0
S31	SPHT1 LTSH	ECON1	49.4167	98.8366	804.3419	631.093	0
S32	ECON1	HX2 secon	49.4167	98.8366	677.5327	467.9275	0
S33	HX1 primary	EXH1	49.4167	98.8366	566.6161	329.751	1
S34	C1 primary	HX1 primary	10.8308	113.9746	319.6148	31.8897	1
S35	FWH4 LPH2	FWH3 LPH1	27.7811	630.6625	357.1063	351.9847	0
S36	FWH3 LPH1	FWH4 LPH2	1.2964	175	389.2118	487.0023	0
S37	SPHT1 LTSH	SPHT1 HTSH	31.762	4960.0534	593.8967	2990.6309	1
S4	SPHT1 HTSH	ST1	31.762	4800.5427	675.9078	3208.4795	1
S41	ST2	GEN1	0	0	0	0	0.5
S42	ST1	ST2	27.7811	550	432.486	2760.7951	1

Journal of Applied Engineering Science

Vol. 22, No. 1, 2024

www.engineeringscience.rs

iipp
publishing

Djarot B. Darmadi et al. - Combined impact of primary-secondary ratio and excess air on coal-fired power plant performance

Stream	From	To	Flow	Pressure	Temperature	Enthalpy	Quality
S43	FWH2 HPH2	FWH1 HPH1	32.0797	7172.7827	413.2439	593.9507	0
S5	ST2	CND1	25.1185	18.5416	331.6088	2288.5468	0.8652
S6	ST1	ST2	0	0	0	0	0.5
S7	CND1	PUMP1 CEP	27.7811	18.5416	331.6088	244.6418	0
S8	PUMP1 CEP	FWH4 LPH2	27.7811	1261.325	331.7141	246.1277	0
S9	ST2	FWH4 LPH2	1.3662	79	366.3242	2472.6023	0.9153
Expansion Line End	ST1	ST1	27.7811	550	432.486	2760.7951	1
Internal Pump Flow	PUMP1 CEP	PUMP1 CEP	27.7811	18.5416	331.6088	244.6417	0
Internal Pump Flow	PUMP2 BFP	PUMP2 BFP	32.0797	177.97	389.7317	489.2079	0
Expansion Line End	ST2	ST2	25.1185	18.5416	331.6088	2288.5468	0.8652

Nomenclature			Subscripts		
	$\dot{m}$	Mass flow	ar		Ash received
	W	Work	c		Coal
	Q	Heat duty	in		Inlet
	η	Efficiency	out		Outlet
	T	Temperature	stoic		Stoichiometric
	LHV	Lower heating value	fg		Flue gas
	λ	Air to fuel stoichiometric ratio	evap		Evaporator
	DAF	Dry ash free			
	LTSH	Low temperature superheater			
	HTSH	High temperature superheater			
	Econ	Economizer			
	PAH	Primary air heater			
	SAH	Secondary air heater			
	DEA	Deaerator			